Published in final edited form as:
Hepatology. 2013 June ; 57(6): 2213–2223. doi:10.1002/hep.26285.

Selective hepatic insulin resistance in mice heterozygous for a mitochondrial trifunctional protein defect

R. Scott Rector[1,2,3], **E. Matthew Morris**[1,2], **Suzanne Ridenhour**[1,2], **Grace M. Meers**[1,2], **Fong-Fu Hsu**[5], **John Turk**[5], and **Jamal A. Ibdah**[1,2,3,4]

[1]Harry S Truman Memorial Veterans Medical Center, Columbia, Missouri 65212, USA

[2]Department of Internal Medicine-Division of Gastroenterology and Hepatology, University of Missouri

[3]Department of Nutrition and Exercise Physiology, University of Missouri

[4]Department of Medical Pharmacology and Physiology, University of Missouri

[5]Department of Internal Medicine, Mass Spectrometry Resource, Division of Endocrinology, Diabetes, Metabolism, and Lipid Research, Washington University School of Medicine, St. Louis, MO 63110, USA

Abstract

Earlier reports suggest a link between mitochondrial dysfunction and development of hepatic insulin resistance. Here we used a murine model heterozygous (HET) for a mitochondrial trifunctional protein (MTP) gene defect to determine if a primary defect in mitochondrial long-chain fatty acid oxidation disrupts hepatic insulin action. Hyperinsulinemic-euglycemic clamps and signaling studies were performed for assessment of whole-body and hepatic insulin resistance/signaling. In addition, hepatic fatty acid oxidation and hepatic insulin action were assessed in vitro utilizing primary hepatocytes isolated from HET and wild-type (WT) mice. In both hepatic mitochondria and isolated primary hepatocytes, heterozygosity of MTP caused a ~50% reduction in mitochondrial fatty acid oxidation, a significantly impaired glucose disposal during the insulin clamp, and a markedly lower insulin-stimulated suppression of hepatic glucose production. HET mice also exhibited impaired insulin signaling, with increased hepatic phosphorylation of IRS2 (ser731) and reduced Akt phosphorylation (ser473) in both hepatic tissue and isolated primary hepatocytes. Assessment of insulin-stimulated FOXO1/phospho-FOXO1 protein content and PEPCK/G6Pase mRNA expression did not reveal differences between HET and WT mice. However, insulin-induced phosphorylation of GSK3β was significantly blunted in HET mice. Hepatic insulin resistance was associated with an increased methylation status of the catalytic subunit of protein phosphatase 2A (PP2A-C), but was not associated with differences in hepatic DAG content, activated PKC-ε, IKK-β, JNK, or phospho-JNK protein contents. Surprisingly, hepatic ceramides were significantly lower in the HET mice compared with WT.

Address of Correspondence: R. Scott Rector, PhD, Assistant Professor and Research Health Scientist, Harry S Truman Memorial VA Hospital, Department of Internal Medicine - Division of Gastroenterology and, Hepatology and Department of Nutrition and Exercise Physiology, University of Missouri-Columbia, Columbia, MO 65212, Tel: 573-884-0979, Fax: 573-884-4595, rectors@health.missouri.edu.

Conflicts of Interest: The authors have no conflicts of interest to disclose.

Involved in the study concept and design (RSR, EMM, JAI); acquisition of data (RSR, EMM, SR, GMM, FFH, JT, JAI); analysis and interpretation of data (RSR, EMM, SR, GMM, FFH, JT, JAI); drafting of the manuscript (RSR, JAI); critical revision of the manuscript for important intellectual content (RSR, EMM, SR, GMM, FFH, JT, JAI); statistical analysis (RSR, GMM); obtained funding (RSR, JAI, JT, EMM).

Conclusions—Our data document that a primary defect in mitochondrial fatty acid β-oxidation causes hepatic insulin resistance selective to hepatic glycogen metabolism that is associated with elevated methylated PP2A-C, but independent of other mechanisms commonly considered to be responsible for insulin resistance.

Keywords

mitochondrial function; hepatic insulin resistance; mitochondrial trifunctional protein

Introduction

Despite the fact that nonalcoholic fatty liver disease (NAFLD) and insulin resistance are strongly associated,[1] a unifying pathophysiology between them remains poorly understood. Recent work by our group and others suggests that hepatic mitochondrial dysfunction may be an initial event in liver lipid accumulation[2, 3] and intimately linked to the development of hepatic insulin resistance.[4, 5] In addition, there are clear associations between hepatic steatosis and hepatic insulin resistance, [6, 7] and it is believed by some that hepatic insulin resistance may precede peripheral insulin resistance.[8] These studies raise the possibility that mitochondrial dysfunction could be a cause, effect or a concurrent feature in insulin resistance. An intriguing hypothesis is that reduced hepatic mitochondrial content/function is a primary cause for development of hepatic insulin resistance.

Hepatic insulin action to regulate hepatic glucose output is mediated through activation of the insulin receptor, insulin receptor substrates (IRS-1 & -2), phosphatidylinositol 3-kinase, and Akt pathway. Under normal insulin-sensitive conditions, insulin inhibits glycogenolysis and gluconeogenesis, suppressing glucose production.[9] However, in the insulin-resistant state, defects in hepatic insulin signaling are thought to be present, impairing insulin-suppression of hepatic glucose production, leading to hyperglycemia and compensatory hyperinsulinemia.[6] The main outcome of hepatic insulin resistance is unrestrained hepatic glucose production either through decreased glycogen synthesis or failure to appropriately suppress hepatic gluconeogenesis.[10]

The mechanisms responsible for disruption of hepatic insulin signaling in the insulin resistant state are under intense investigation. It has been observed by some that increased inflammation and oxidative stress are present in conjunction with hepatic insulin resistance.[11] Whereas, others suggest that lipid metabolites/intermediates, such as diacylglycerols (DAGs) and ceremides, are determinants for the development of insulin resistance (reviewed by[12–14]). Collectively, the mechanism(s) responsible for blunted hepatic insulin action are not definitively known.

To address the relationship between hepatic mitochondrial dysfunction, reduced hepatic insulin action, and the potential mechanism(s), we have utilized a murine model heterozygous (HET) for a mitochondrial trifunctional protein (MTP; the enzyme complex responsible for catalyzing the critical last three steps in long-chain fatty acid β-oxidation) gene defect previously generated by our group.[2] HET-MTP mice exhibit a ~50% reduction in hepatic MTP protein expression and develop hepatic steatosis and systemic insulin resistance in part due to impaired mitochondrial long-chain fatty acid oxidation.[2] Our novel MTP mouse model offers a unique opportunity to gain insight into the role of mitochondria in development of hepatic insulin resistance. Here, we sought to test our hypothesis that a primary defect in mitochondrial β-oxidation disrupts hepatic insulin action both in vivo and in vitro utilizing primary hepatocytes. Furthermore, we examined potential key mechanistic causes of disruption in hepatic insulin signaling, including assessment of hepatic

inflammatory pathways, as well as measurement of hepatic DAG and ceramide content and phosphatases involved in hepatic insulin signaling.

METHODS

Animal protocol

The animal protocol was approved by the Institutional Animal Care and Use Committee at the University of Missouri–Columbia. Male $MTP^{+/+}$ (WT) and $MTP^{+/-}$(HET) mice were generated and genotype was determined by PCR using primers that distinguish the mutant allele from the wild-type allele as previously described.[2, 15] Cages were in temperature-controlled animal quarters (21°C) with a 06.00–18.00 h light: 18.00–06.00 h dark cycle that were maintained throughout the experimental period. All animals were provided standard rodent chow (Formulab 5008, Purina Mills, St Louis, MO, USA) with weekly cage changes during which body mass and food intake was obtained. Mice were anesthetized [sodium pentobarbital (100 mg·kg−1)] following a 5 hr fast and killed by exsanguination by removal of the heart. For acute insulin stimulation studies, food was removed 5 hrs before mice were given an intraperitoneal injection of insulin (Humulin, 2.5 U/kg) and tissues were harvested under anesthesia 20 minutes post injection.

Hepatocyte isolation and culture

Hepatocytes from 12 month old mice were isolated by collagenase perfusion and cultured for 5 days in a thin-layer collagen matrix as previously described with minor changes.[16, 17] On the day of experiments, cells were serum starved for 5 hrs. Cells for determination of insulin action were stimulated with 150 nM insulin for 15 minutes, lysed, and frozen at −80°C. All data was generated in 6 to 8 experiments (n=6–8); each experiment was performed using primary hepatocytes isolated from individual animals.

Hepatic mitochondria isolation and fatty acid oxidation

Mitochondrial suspensions were prepared according to modified methods of Koves et al [18] as described previously by our group.[19] Palmitate oxidation ($^{14}CO_2$, representing complete fatty acid oxidation was measured with radiolabeled [1-^{14}C]palmitate (American Radiochemicals) in freshly isolated liver mitochondria and in serum starved primary hepatocytes as previously described.[17, 19–21]

Analysis of intrahepatic lipid content, liver histology, and hepatic content of glycogen, diacylglycerols, and ceramides

Intrahepatic lipids were extracted, quantified, and expressed as nmol/g tissue wet weight as previously described.[20] Hepatic DAG content was determined after TLC isolation by methanolysis and measurement of fatty acid methyl esters by gas chromatography with flame ionization detection, as previously described by our group.[22] Hepatic glycogen content was assessed as previously described by our group.[20] Hepatic ceramides were extracted by the method of Bligh and Dyer.[23] Ceramide (Cer) species were measured relative to a C8:0-Cer internal standard by negative-ion ESI/MS/MS analysis (as $[M - H]^-$ ions) employing neutral loss of 256 with a Thermo TSQ Vantage triple quadrupole instrument (San Jose, CA) as previously described,[24] and normalized to sample protein content.

Hyperinsulinemic-Euglycemic clamp

Hyperinsulinemic-euglycemic clamps were performed in conscious mice following a 5 hour fast as previously described.[25] After mice were anesthetized with sodium pentobarbital (50–75 mg/kg), the left common carotid artery and the right jugular vein were catheterized, free

ends of catheters tunneled under the skin to the back of the neck where they were exteriorized and sealed with stainless steel plugs. Experiments were performed when mice were within 2 g of pre-surgery weight (~5 days). Baseline blood samples were taken, followed by a priming bolus (1 μCi) and then a constant infusion (0.05 μCi/min) of ^{3}H-3-glucose for a 2 hour period and a second blood sample was taken to assess basal hepatic glucose output. A priming bolus of insulin (16 mU/kg) was given and a constant infusion of insulin (4mU/kg/min) and glucose (50g/100ml) infusion rate was adjusted to maintain euglycemia. In addition, a constant infusion of ^{3}H-3-glucose (0.1 μCi/min) was maintained to measure insulin-suppression of hepatic glucose output. Mice received saline-washed erythrocytes from donors throughout (5–6 μl/min) to prevent a fall of >5% hematocrit. At the end of clamps, the animals were anesthetized and liver was taken and frozen immediately. Rates of whole-body glucose appearance and uptake were determined as the ratio of the [^{3}H]glucose infusion rate to the specific activity of plasma glucose during the final 40 minutes of clamps. Hepatic glucose production during the clamps was determined by subtracting the glucose infusion rate from the whole-body glucose appearance.

Western blot analyses

Western blot analyses were performed for the determination of forkhead box O1 (FoxO1), phospho-FoxO1 Ser^{256}, glycogen synthase kinase-3β (GSK-3β), phospho-GSK-3β Ser^{9}, glycogen synthase (GS), phospho-GS Ser641, protein kinase B (Akt), phospho-Akt Ser^{473}, c-Jun N-terminal kinase (JNK), phospho-JNK Thr^{133}/Tyr^{185}, rapamycin-insensitive companion of mTOR (RICTOR), phospho-RICTOR Thr^{1135}, regulatory-associated protein of mTOR (RAPTOR), phospho-RAPTOR Ser792, p70S6 kinase, phospho-p70S6K Thr389, S6 Ribosomal Protein (S6), phospho-S6 Ser240/244, phosphatase and tensin homologue deleted on chromosome ten (PTEN), phospho-PTEN Ser380/Thr382/383, insulin receptor substrate-2 (IRS-2) [all from Cell Signaling, Beverly, MA], phospho-IRS-2 Ser^{731} (Abcam, Cambridge, MA), inhibitor κB kinase β (IKKβ; Cell Signaling), protein kinase C-ε (PKC-ε; Millipore, Temecula, CA), anti-methyl-type 2 protein serine/threonine phosphatase subunit C (methyl-PP2A-C; Millipore), and PH domain leucine-rich repeat protein phosphatase (PHLPP1 and 2; Bethyl Lab, Inc, Montgomery, TX). Content of phospho-proteins(using phospho-specific antibodies) was calculated from thedensity of the band of the phospho-protein divided by the densityof the protein (total) using the appropriate antibody.[20, 26] To examine hepatic PKCε membrane translocation and activation status, membrane and cytosol protein extracts were performed as previously described[27] and western blot analyses for PKCε were performed as described above. In order to control and correct for equal protein loading and transfer, the membraneswere stained with 0.1% amido-black (Sigma) and total protein staining was quantified.[20]

Fat pad collection and serum assays

Retroperitoneal and epididymal adipose tissue fat pads were removedfrom exsanguinated animals and weighed. Serum glucose (Sigma, St. Louis, MO, USA), TAG (Sigma, St. Louis, MO, USA), free fattyacids (FFA;Wako Chemicals, Richmond, VA, USA), and insulin (Linco Research,St. Charles, MO, USA) were measured using commercially availablekits according to the manufacturer's instructions.

Superoxide dismutase (SOD), catalase, citrate synthase, Beta-hydroxyacyl-CoA dehydrogenase (β-HAD), and glutathione reductase activity

SOD and catalase activity in liver homogenate was determined by commercially available methods (Cayman Chemicals, Ann Arbor, MI, USA and Sigma). Citrate synthase and β-HAD activities were determined using the methods of Srere et al [28] and Bass et al,[29] respectively, as previously described.[20, 26]

Quantitative RT-PCR

PEPCK and G6Pase mRNA expression was quantified by RT-PCR using the ABI 7500 Fast Sequence Detection System and software with commercially available primers with techniques previously described by our group.[17] Results were quantified using the DdC_T method relative to cyclophilin b or GAPDH.

Statistics

Each outcome measure was examined in 8–12 animals per group. Fatty acid oxidation experiments in isolated primary hepatocytes were performed in 6–7 animals per group. For each outcome measure, an independent samples t-test was (SPSS/15.0, SPSS, Chicago, IL, USA). Values are reported as means ± standard error of the mean (SE), and a P value less than 0.05 denotes a statistically significant difference.

RESULTS

Animal characteristics and fatty acid oxidation

Body weight and fat pad mass of both epididymal and retroperitoneal fat were 10–15% lower in HET compared with WT animals ($p<0.01$, Table 1), while food consumption did not differ between groups. Following a 5 hr fast, serum TAGs, FFAs, insulin, glucose, ALTs, and β-hydroxy-butrate did not differ between HET and WT animals (Table 1). In addition, hepatic SOD-1, catalase, β-HAD, and citrate synthase activity did not differ between groups (Table 1). Heterozygosity for the MTP was confirmed, with HET mice exhibiting a ~50% reduction in MTP α-subunit protein content ($p<0.01$, Figure 1A), and HET MTP mice also had a 50% reduction in mitochondrial fatty acid oxidation in liver and in primary hepatocytes compared with WT mice (complete palmitate oxidation to CO_2, $p<0.05$, Figure 1B and 1C).

Systemic and hepatic insulin resistance during hyperinsulinemic-euglycemic clamp

Euglycemia was maintained in both HET and WT mice during the two hour clamp procedure and did not differ statically between groups (Figure 2A), but it required a significantly greater glucose infusion in the WT vs. HET mice, as shown in figure 2A and during the final 40 minutes of insulin clamp ($p=0.02$, Figure 2B). HET mice also exhibited a markedly lower insulin-induced suppression of hepatic glucose production (10% vs. 50% suppression, respectively, $p=0.037$, Figure 2C).

Insulin signaling

The blunted insulin suppression of hepatic glucose output was associated with impaired hepatic insulin signaling in the HET MTP mice, including a 60% increase in phosphorylation of IRS2 at Ser731 (Figure 3A, $p<0.01$) and a −70% reduction in Akt Ser473 phosphorylation ($p<0.01$) in HET compared with WT animals following the hyperinsulinemic clamp. These impairments were further confirmed following acute insulin stimulation, with increased IRS-2 Ser731 phosphorylation and reduced Akt Ser473 phosphorylation in the HET mice ($p<0.05$, Figure 3B). In addition, when primary hepatocytes were examined in isolation from other systemic factors, the impairment in insulin signaling was also present at the level of Akt phosphorylation (Figure 3C, $p<0.05$).

Further downstream examination of the insulin signaling cascade revealed no difference in the insulin-stimulated changes in FOXO1 or phospho-FOXO1 (Ser 256) between the HET and WT groups; whereas, total FOXO1 protein content was significantly elevated in the HET MTP mice in the basal state compared with WT ($p<0.01$, Figure 4A). In addition, while G6Pase mRNA expression was significantly higher in the WT vs. HET mice under

basal conditions, hepatic PEPCK or G6Pase mRNA expression did not differ in the insulin-stimulated state between the HET and WT mice (Figure 4B). However, the insulin stimulated increase in phosphorylated GSK3β was significantly blunted in HET compared with WT mice (Figure 4C, 50% lower pGSK3β/GSK3β, $p<0.05$). This reduced ability to regulate GSK3β activity resulted in increased GS phosphorylation (Figure 4D, $p<0.05$) and lower hepatic glycogen content in the HET (Figure 4E, $p=0.02$) following the 2 h hyperinsulinemic-euglycemic clamp. Collectively, these results suggest that the impairment in insulin suppression of hepatic glucose output observed in the HET MTP mouse is likely due to impairment in glycogen synthesis rather than dysregulation in the hepatic gluconeogenesis pathway.

Potential mechanisms responsible for blunted hepatic insulin action in the HET MTP mice

As we have previously reported[2], heterozygosity for MTP results in significant elevations in hepatic TAG content compared with WT animals (Figure 5A, $p<0.05$). However, examination of hepatic DAG content revealed no significant differences in total, saturated, or unsaturated DAG species between HET and WT mice (Figure 5B). In addition, hepatic JNK, phospho-JNK, and IKKβ protein content did not differ between genotypes (Figure 5C). Moreover, hepatic PKCε protein expression did not differ in the basal or insulin-stimulated state at either the membrane or in the cytosol, suggesting that PKCε activation status of HET and WT mice did not differ (Figure 5D). Surprisingly, hepatic ceramide content (total, saturated, unsaturated, and individual species) of HET mice was significantly lower than that of the WT mice (Figure 5E, $p<0.05$). Further examination of phosphatases known to alter Akt activation revealed that the amount of activated (methylated) protein phosphatase 2A subunit C (methyl-PP2A–C) was significantly elevated in the HET compared with WT mice in the insulin-stimulated condition ($p<0.05$), but no differences for PTEN, phospho-PTEN (Ser380/Thr382/Thr383), PHLPP1, or PHLPP2 (Figure 5F). Moreover, no differences were found between WT and HET mice for RAPTOR, phospho-RAPTOR(Ser792), p70S6K, phospho-p70S6K (Thr389), S6, phospho-S6 (Ser240/244), RICTOR, or phospho-RICTOR (Thr1135) following the hyperinsulinemic clamp (data not shown).

DISCUSSION

Evidence is mounting that mitochondrial dysfunction may be intimately linked to the development of hepatic insulin resistance. Here we report that a primary heterozygous genetic defect in mitochondrial trifunction protein (MTP) reduces fatty acid oxidation in isolated hepatic mitochondria and in primary hepatocytes and leads to hepatic insulin resistance in vivo and in vitro in a non-obese, non-high fat fed mouse model. The hepatic insulin resistance witnessed in the MTP heterozygous mice was not associated with excess accumulation in hepatic DAGs, ceramides or the activation status of PKCε, nor in the elevation of hepatic inflammatory pathways, but was related to increases in protein phosphatase 2A. Moreover, while dysregulated hepatic insulin signaling was observed at the level of IRS-2 and Akt, blunted insulin signaling was selective towards glycogen storage, but not gluconeogenesis.

MTP defects were first reported in humans in 1992.[30] While complete MTP deficiency occurs in about 1:38,000 pregnancies, it is estimated that 2%–3% of the US population is heterozygous for a defect in mitochondrial fatty acid oxidation (reviewed in [31]). Heterozygosity for mitochondrial fatty acid defects causes inefficient mitochondrial β-oxidation, a progressive accumulation of intra-hepatic fatty acids, and NAFLD. We have previously reported that complete MTP deficiency results in neonatal sudden death, with mouse fetuses accumulating serum long-chain acylcarnitines and 3-hydroxy acylcarnitines, as well as hepatic long-chain fatty acids similar to the human deficiency.[15] In addition, low-

fat fed HET-MTP mice develop hepatic steatosis and systemic insulin resistance at 9–10 months of age, and display mildly elevated long-chain hepatic fatty acids, elevated superoxide dismutase and glutathione peroxidase activities, and reduced glutathione levels at 14–18 months of age.[2] In this report, we utilized this well characterized mouse model to explore the link between mitochondrial dysfunction and hepatic insulin resistance. Our clamp studies revealed reduced insulin suppression of hepatic glucose production, documenting hepatic insulin resistance in these animals. Moreover, the phenotype of marked blunting in insulin-induced Akt phosphorylation was maintained in isolated primary hepatocytes, eliminating the influence of other systemic factors and tightening the link between reduced hepatic fatty acid oxidation and hepatic insulin resistance.

Hepatic insulin resistance are thought to include both decreased glycogen synthesis and/or decreased suppression of glycogenolysis, as well as the failure to effectively suppress gluconeogenesis.[9, 10] Hepatic glucose output is mediated through activation of IR, IRS-1 & -2, PI3-K and Akt by insulin, and once activated through phosphorylation, Akt can promote increases in glycogen content by activating glycogen synthase through the inhibition (phosphorylation) of GSK3β.[32] In addition, under insulin-stimulated conditions, Akt phosphorylates FOXO1 (key transcriptional regulator of PEPCK and G6Pase) on Ser^{256}, which triggers its nuclear exclusion into the cytoplasm and reduces transcription of the gluconeogenic genes.[33, 34] HET-MTP mice appeared to have normal insulin-induced regulation of the gluconeogenic factors FOXO1, PEPCK, and G6Pase. However, insulin-induced phosphorylation of GSK-3β was blunted, insulin-induced phosphorylation of glycogen synthase was elevated, and hepatic glycogen content following the clamp was significantly lower in the HET-MTP mice. These novel findings suggest that the reduced insulin suppression of hepatic glucose output observed during the hyperinsulinemic-euglycemic clamp may be selective to impaired hepatic glycogen metabolism and not gluconeogenesis. Another example of selective insulin resistance in liver is where there is failure to suppress glucose output, but continued or enhanced activation of lipogenesis (see recent commentary[35]).

We examined the most plausible candidates for the observed disruption in insulin suppression of hepatic glucose output and blunted insulin signaling seen in the HET-MTP mice. IKK and JNK pathway activation can blunt Akt activation and cause insulin resistance,[36, 37] and ceramide accumulation also has been implicated in the development of hepatic insulin resistance, [11] with activation of IKK and NF-κB triggering ceramide synthesis and blunting Akt signaling.[11] Here we report that reductions in mitochondrial fatty acid oxidation were associated with reduced Akt phosphorylation, although hepatic ceramide content was actually lower for HET-MTP than for WT mice. In addition, there was no apparent activation in the JNK and NF-κB pathways, as indicated by the lack of differences between genotypes in JNK, phospho-JNK, or IKK-β.

Hepatic DAGs are thought to activate classic and atypical PKCs and blunt insulin signaling at the insulin receptor and insulin receptor substrate.[13] There are numerous studies implicating hepatic DAGs in potentially causing hepatic insulin resistance;[38–42] although, several recent studies refute DAGs role (see recent perspectives[13, 14]). While we observed dysregulated insulin signaling at IRS-2 (phosphorylation at Ser731 is counter regulatory) and Akt, DAGs were not elevated in HET mice. In addition, PKCε (the predominant isoform activated in the liver[13]) activation was not increased. Similar to our findings, deficiency in long chain acyl-CoA dehydrogenase ($LCAD^{-/-}$) results in hepatic insulin resistance,[4] which the authors attributed to PKCε activation due to elevated hepatic DAG synthesis during insulin stimulation. However, in humans, LCAD is a redundant enzyme and apparently has a limited role in mitochondrial long chain fatty acid oxidation, and to date, there are no reports of its deficiency. Unfortunately, we did not assess hepatic DAG content

after the hyperinsulinemic-euglycemic clamp due to radio-labeled tracer used during the procedures, but we did not see increases in activated PKCε (PKCε found in the membrane) following the insulin clamp, suggesting the lack of elevation in hepatic DAGs after insulin infusion and reducing the likelihood of DAGs as a cause for hepatic insulin resistance in this animal model.

Due to the lack of differences in hepatic DAGs, ceramides, and the activation status of PKCε or JNK/IKKβ, we performed extensive examination of proteins involved in the mTOR pathway (RAPTOR, RICTOR, S6, S6 kinase) and found no differences between WT and HET mice. However, examination of phosphatases known to play a role in the regulation of insulin signaling (PTEN, PHLPP1&2, and PP2A) revealed an increase in the methylation status of the catalytic subunit of PP2A in the HET mice. Methylation of the catalytic subunit is required for the activation of the PP2A enzyme,[43] and it has been recently reported that palmitate-induced insulin resistance in hepatocytes is mediated through increased methylation and activation of PP2A and downregulation of Akt phosphorylation.[44] These findings suggest that accumulation of other lipid metabolites and/or fatty acids due to disrupted mitochondrial β-oxidation causes hepatic insulin resistance perhaps in part through methylation and activation of PP2A. Future investigation into the role of PP2A in the setting of mitochondrial dysfunction and what regulates PP2A methylation status are warranted.

Our findings do not exclude the possibility that particular DAGs species and/or localization may be linked to insulin resistance or that other novel PKCs may be upregulated.[45] Moreover, long-chain acyl-CoAs may have contributed to hepatic insulin resistance in the HET-MTP mice. Perhaps a future metabolomics approach is needed to identify other metabolite(s) involved in the disruption of hepatic insulin signaling.

In summary, we demonstrate that a primary defect in mitochondrial long-chain fatty acid β-oxidation impairs systemic glucose disposal, blunts hepatic insulin signaling, and contributes to hepatic insulin resistance in the absence of high fat feeding or obesity. This observed hepatic phenotype is maintained *in vitro* in isolated primary hepatocytes, independent of peripheral factors. In addition, the hepatic insulin resistance was associated with an increased amount of methylated PP2A–C, but not with differences in hepatic DAGs, ceramides, the activation status of PKCε, or hepatic inflammatory pathways (JNK and IKKβ). Moreover, with the findings of selective insulin resistance towards improper hepatic glycogen handling and not dysregulation in gluconeogenesis, the role of hepatic glycogen metabolism should be considered as we look to develop better therapeutics for the management of fatty liver disease and insulin resistance.

Acknowledgments

This work was supported by NIH grants DK-56345 (JAI), F32 DK-83182 (RSR), P41-RR00954 (JT), P60-DK20579 (JT), P30-DK56341 (JT), and T32 AR 048523-07 (EMM) and Veterans Affairs grant VHA-CDA2 IK2BX001299-01 (RSR) and by institutional funds from University of Missouri School of Medicine.

The authors would like to thank Craig Meers, Raad Gitan, and Meghan Ruebel for excellent technical assistance to this work, and the Veterinary Medicine Diagnostics Laboratory at the University of Missouri for help with the histological sections and serum ALT measurements. In addition, the authors would like to thank Dr. John Thyfault for his intellectual input to this work, and we would like to thank Dr. David Wasserman, Dr. Owen McGuinness, and the MMPC staff at Vanderbilt University for technical assistance and training with the euglycemic clamp procedures. This work was supported with resources and the use of facilities at the Harry S Truman Memorial Veterans Hospital in Columbia, MO.

Abbreviations

ALT	alanine aminotransferase
β-HAD	Beta-hydroxyacyl-CoA dehydrogenase
FFA	free fatty acids
NAFLD	non-alcoholic fatty liver disease
MTP	mitochondrial trifunction protein
TAG	triacylglycerol

References

1. Rector RS, Thyfault JP, Wei Y, et al. Non-alcoholic fatty liver disease and the metabolic syndrome: An update. World J Gastroenterol. 2008; 14:185–92. [PubMed: 18186553]
2. Ibdah JA, Perlegas P, Zhao Y, et al. Mice heterozygous for a defect in mitochondrial trifunctional protein develop hepatic steatosis and insulin resistance. Gastroenterology. 2005; 128:1381–90. [PubMed: 15887119]
3. Rector RS, Thyfault JP, Uptergrove GM, et al. Mitochondrial dysfunction precedes insulin resistance and hepatic steatosis and contributes to the natural history of non-alcoholic fatty liver disease in an obese rodent model. J Hepatol. 2010; 52:727–36. [PubMed: 20347174]
4. Zhang D, Liu ZX, Choi CS, et al. Mitochondrial dysfunction due to long-chain Acyl-CoA dehydrogenase deficiency causes hepatic steatosis and hepatic insulin resistance. Proc Natl Acad Sci U S A. 2007; 104:17075–80. [PubMed: 17940018]
5. Patti ME, Corvera S. The role of mitochondria in the pathogenesis of type 2 diabetes. Endocr Rev. 2010; 31:364–95. [PubMed: 20156986]
6. Marchesini G, Brizi M, Morselli-Labate AM, et al. Association of nonalcoholic fatty liver disease with insulin resistance. Am J Med. 1999; 107:450–5. [PubMed: 10569299]
7. Clark JM, Diehl AM. Hepatic steatosis and type 2 diabetes mellitus. Curr Diab Rep. 2002; 2:210–5. [PubMed: 12643175]
8. Perseghin G. Viewpoints on the way to a consensus session: where does insulin resistance start? The liver Diabetes Care. 2009; 32 (Suppl 2):S164–7.
9. Dentin R, Liu Y, Koo SH, et al. Insulin modulates gluconeogenesis by inhibition of the coactivator TORC2. Nature. 2007; 449:366–9. [PubMed: 17805301]
10. Leclercq IA, Da Silva Morais A, Schroyen B, et al. Insulin resistance in hepatocytes and sinusoidal liver cells: mechanisms and consequences. Journal of hepatology. 2007; 47:142–56. [PubMed: 17512085]
11. Bikman BT, Summers SA. Ceramides as modulators of cellular and whole-body metabolism. J Clin Invest. 2011; 121:4222–30. [PubMed: 22045572]
12. Postic C, Girard J. Contribution of de novo fatty acid synthesis to hepatic steatosis and insulin resistance: lessons from genetically engineered mice. J Clin Invest. 2008; 118:829–38. [PubMed: 18317565]
13. Jornayvaz FR, Shulman GI. Diacylglycerol activation of protein kinase cepsilon and hepatic insulin resistance. Cell Metab. 2012; 15:574–84. [PubMed: 22560210]
14. Farese RV Jr, Zechner R, Newgard CB, et al. The Problem of Establishing Relationships between Hepatic Steatosis and Hepatic Insulin Resistance. Cell Metab. 2012; 15:570–3. [PubMed: 22560209]
15. Ibdah JA, Paul H, Zhao Y, et al. Lack of mitochondrial trifunctional protein in mice causes neonatal hypoglycemia and sudden death. J Clin Invest. 2001; 107:1403–9. [PubMed: 11390422]
16. Gugen-Guillouzo, C. Isolation and Culture of Animal and Human Hepatocytes. In: Freshney, RI.; Freshney, MG., editors. Culture of Epithelial Cells. 2. Wiley-Liss; 2002. p. 337-379.

17. Morris EM, Meers GM, Booth FW, et al. PGC-1alpha Overexpression Results in Increased Hepatic Fatty Acid Oxidation with Reduced Triacylglycerol Accumulation and Secretion. Am J Physiol Gastrointest Liver Physiol. 2012
18. Koves TR, Noland RC, Bates AL, et al. Subsarcolemmal and intermyofibrillar mitochondria play distinct roles in regulating skeletal muscle fatty acid metabolism. Am J Physiol Cell Physiol. 2005; 288:C1074–82. [PubMed: 15647392]
19. Thyfault JP, Rector RS, Uptergrove GM, et al. Rats selectively bred for low aerobic capacity have reduced hepatic mitochondrial oxidative capacity and susceptibility to hepatic steatosis and injury. J Physiol. 2009; 587:1805–16. [PubMed: 19237421]
20. Rector RS, Thyfault JP, Morris RT, et al. Daily exercise increases hepatic fatty acid oxidation and prevents steatosis in Otsuka Long-Evans Tokushima Fatty rats. Am J Physiol Gastrointest Liver Physiol. 2008; 294:G619–26. [PubMed: 18174272]
21. Muoio DM, Way JM, Tanner CJ, et al. Peroxisome proliferator-activated receptor-alpha regulates fatty acid utilization in primary human skeletal muscle cells. Diabetes. 2002; 51:901–9. [PubMed: 11916905]
22. Rector RS, Uptergrove GM, Morris EM, et al. Daily exercise vs. caloric restriction for prevention of nonalcoholic fatty liver disease in the OLETF rat model. Am J Physiol Gastrointest Liver Physiol. 2011; 300:G874–83. [PubMed: 21350190]
23. Bligh EG, Dyer WJ. A rapid method of total lipid extraction and purification. Can J Biochem Physiol. 1959; 37:911–7. [PubMed: 13671378]
24. Hsu FF, Turk J. Characterization of ceramides by low energy collisional-activated dissociation tandem mass spectrometry with negative-ion electrospray ionization. J Am Soc Mass Spectrom. 2002; 13:558–70. [PubMed: 12019979]
25. Ayala JE, Bracy DP, McGuinness OP, et al. Considerations in the design of hyperinsulinemic-euglycemic clamps in the conscious mouse. Diabetes. 2006; 55:390–7. [PubMed: 16443772]
26. Rector RS, Thyfault JP, Laye MJ, et al. Cessation of daily exercise dramatically alters precursors of hepatic steatosis in Otsuka Long-Evans Tokushima Fatty (OLETF) rats. J Physiol. 2008; 586:4241–9. [PubMed: 18617560]
27. Cortright RN, Azevedo JL Jr, Zhou Q, et al. Protein kinase C modulates insulin action in human skeletal muscle. Am J Physiol Endocrinol Metab. 2000; 278:E553–62. [PubMed: 10710511]
28. Srere PA. Citrate synthase. Meth Enzymol. 1969; 13:3–5.
29. Bass A, Brdiczka D, Eyer P, et al. Metabolic differentiation of distinct muscle types at the level of enzymatic organization. Eur J Biochem. 1969; 10:198–206. [PubMed: 4309865]
30. Wanders RJ, LIJ, Poggi F, et al. Human trifunctional protein deficiency: a new disorder of mitochondrial fatty acid beta-oxidation. Biochem Biophys Res Commun. 1992; 188:1139–45. [PubMed: 1445348]
31. Rector RS, Payne RM, Ibdah JA. Mitochondrial trifunctional protein defects: Clinical implications and therapeutic approaches. Adv Drug Deliv Rev. 2008; 60:1488–96. [PubMed: 18652860]
32. Postic C, Dentin R, Girard J. Role of the liver in the control of carbohydrate and lipid homeostasis. Diabetes Metab. 2004; 30:398–408. [PubMed: 15671906]
33. Gross DN, Wan M, Birnbaum MJ. The role of FOXO in the regulation of metabolism. Curr Diab Rep. 2009; 9:208–14. [PubMed: 19490822]
34. Aoyama H, Daitoku H, Fukamizu A. Nutrient control of phosphorylation and translocation of Foxo1 in C57BL/6 and db/db mice. Int J Mol Med. 2006; 18:433–9. [PubMed: 16865227]
35. Brown MS, Goldstein JL. Selective versus total insulin resistance: a pathogenic paradox. Cell Metab. 2008; 7:95–6. [PubMed: 18249166]
36. Hummasti S, Hotamisligil GS. Endoplasmic reticulum stress and inflammation in obesity and diabetes. Circ Res. 2010; 107:579–91. [PubMed: 20814028]
37. Roden M. Mechanisms of Disease: hepatic steatosis in type 2 diabetes--pathogenesis and clinical relevance. Nat Clin Pract Endocrinol Metab. 2006; 2:335–48. [PubMed: 16932311]
38. Jornayvaz FR, Birkenfeld AL, Jurczak MJ, et al. Hepatic insulin resistance in mice with hepatic overexpression of diacylglycerol acyltransferase 2. Proc Natl Acad Sci U S A. 2011; 108:5748–52. [PubMed: 21436037]

39. Kumashiro N, Erion DM, Zhang D, et al. Cellular mechanism of insulin resistance in nonalcoholic fatty liver disease. Proc Natl Acad Sci U S A. 2011; 108:16381–5. [PubMed: 21930939]
40. Samuel VT, Liu ZX, Wang A, et al. Inhibition of protein kinase Cepsilon prevents hepatic insulin resistance in nonalcoholic fatty liver disease. J Clin Invest. 2007; 117:739–45. [PubMed: 17318260]
41. Neuschwander-Tetri BA. Hepatic lipotoxicity and the pathogenesis of nonalcoholic steatohepatitis: The central role of nontriglyceride fatty acid metabolites. Hepatology. 2010; 52:774–88. [PubMed: 20683968]
42. Boden G, She P, Mozzoli M, et al. Free Fatty Acids Produce Insulin Resistance and Activate the Proinflammatory Nuclear Factor-{kappa}B Pathway in Rat Liver. Diabetes. 2005; 54:3458–65. [PubMed: 16306362]
43. Guenin S, Schwartz L, Morvan D, et al. PP2A activity is controlled by methylation and regulates oncoprotein expression in melanoma cells: a mechanism which participates in growth inhibition induced by chloroethylnitrosourea treatment. Int J Oncol. 2008; 32:49–57. [PubMed: 18097542]
44. Galbo T, Olsen GS, Quistorff B, et al. Free fatty acid-induced PP2A hyperactivity selectively impairs hepatic insulin action on glucose metabolism. PLoS One. 2011; 6:e27424. [PubMed: 22087313]
45. Bezy O, Tran TT, Pihlajamaki J, et al. PKCdelta regulates hepatic insulin sensitivity and hepatosteatosis in mice and humans. J Clin Invest. 2011; 121:2504–17. [PubMed: 21576825]

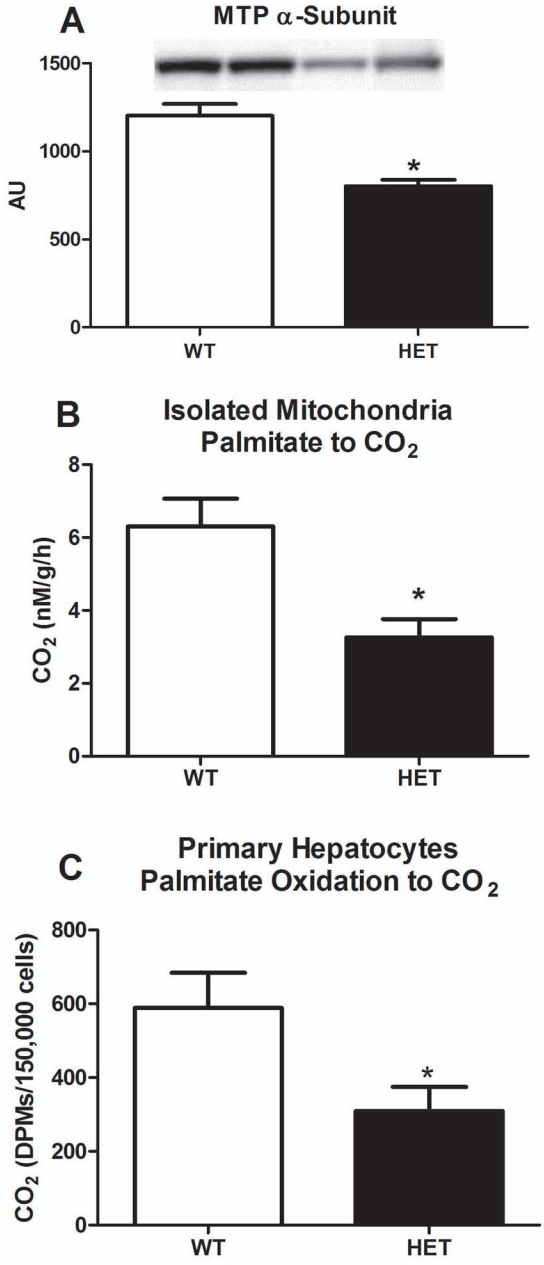

Figure 1.

Hepatic MTP expression and fatty acid oxidation in HET MTP and WT mice. Hepatic MTP α-subunit protein expression (Figure 1A), complete palmitate oxidation to CO_2 in isolated mitochondria from hepatic tissue (Figure 1B), and complete palmitate oxidation to CO_2 in isolated primary hepatocytes (Figure 1C). Values are means ± SE (n=8 per group; n=6 per group for primary hepatocyte work). * Significantly different than WT, $p<0.01$.

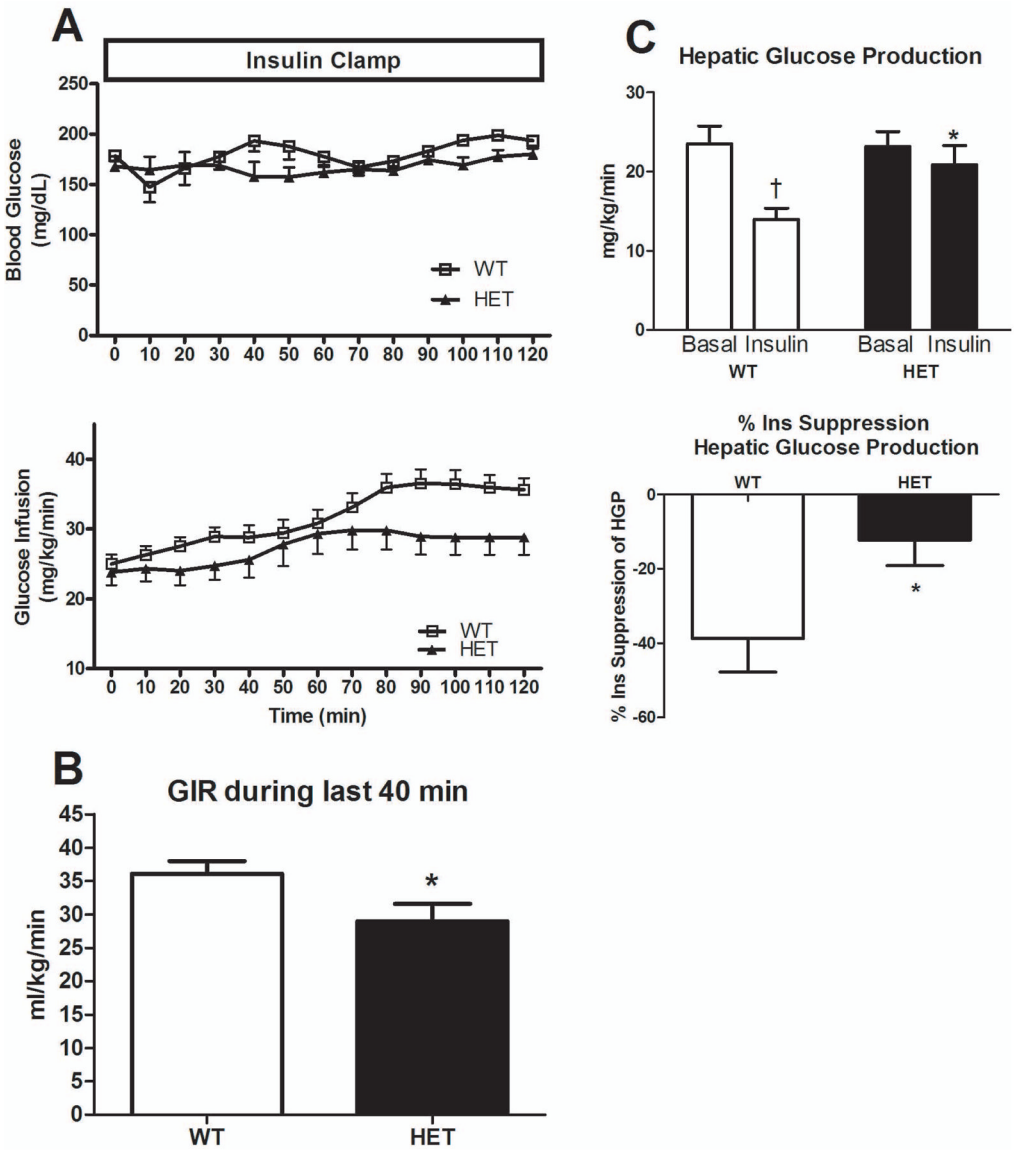

Figure 2.

Hyperinsulinemic-euglycemic clamp data in HET MTP and WT mice. Blood glucose levels and glucose infusion rate to maintain euglycemia (Figure 2A), average glucose infusion rate during the final 40 minutes of clamp (Figure 2B), hepatic glucose production during the basal and insulin stimulated conditions and percent insulin suppression of hepatic glucose output during the clamp (Figure 2C). Values are means ± SE (n=6–8 per group). * Significantly different than WT, $p<0.05$. † Significantly different from basal, $p<0.05$.

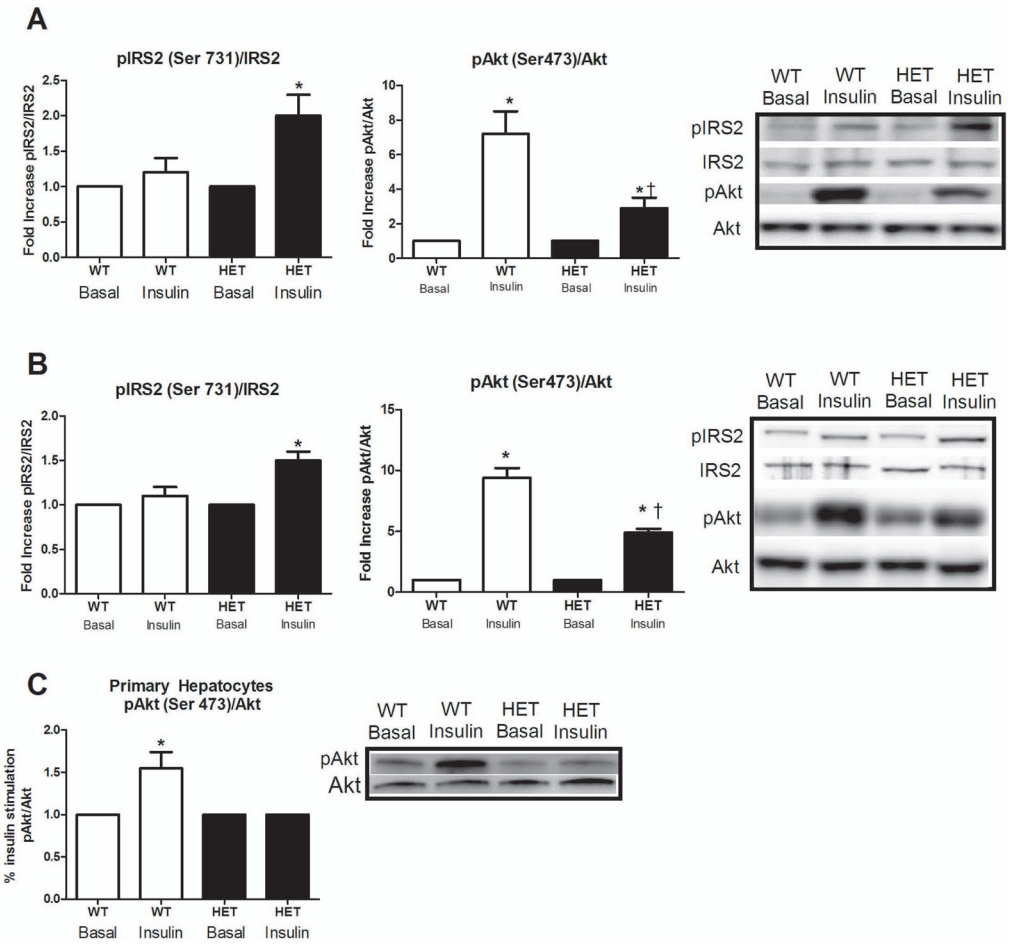

Figure 3.

Hepatic insulin signaling at the level of IRS-2 and Akt in HET MTP and WT mice. IRS-2 and Akt phosphorylation status in the liver under hyperinsulinemic-euglycemic clamp (Figure 3A) and acute insulin stimulated (Figure 3B) conditions and Akt phosphorylation status in isolated primary hepatocytes exposed to acute insulin stimulation (Figure 3C). * Significant difference between basal and insulin stimulation, $p<0.05$. † Significantly different than WT under same condition, $p<0.05$.

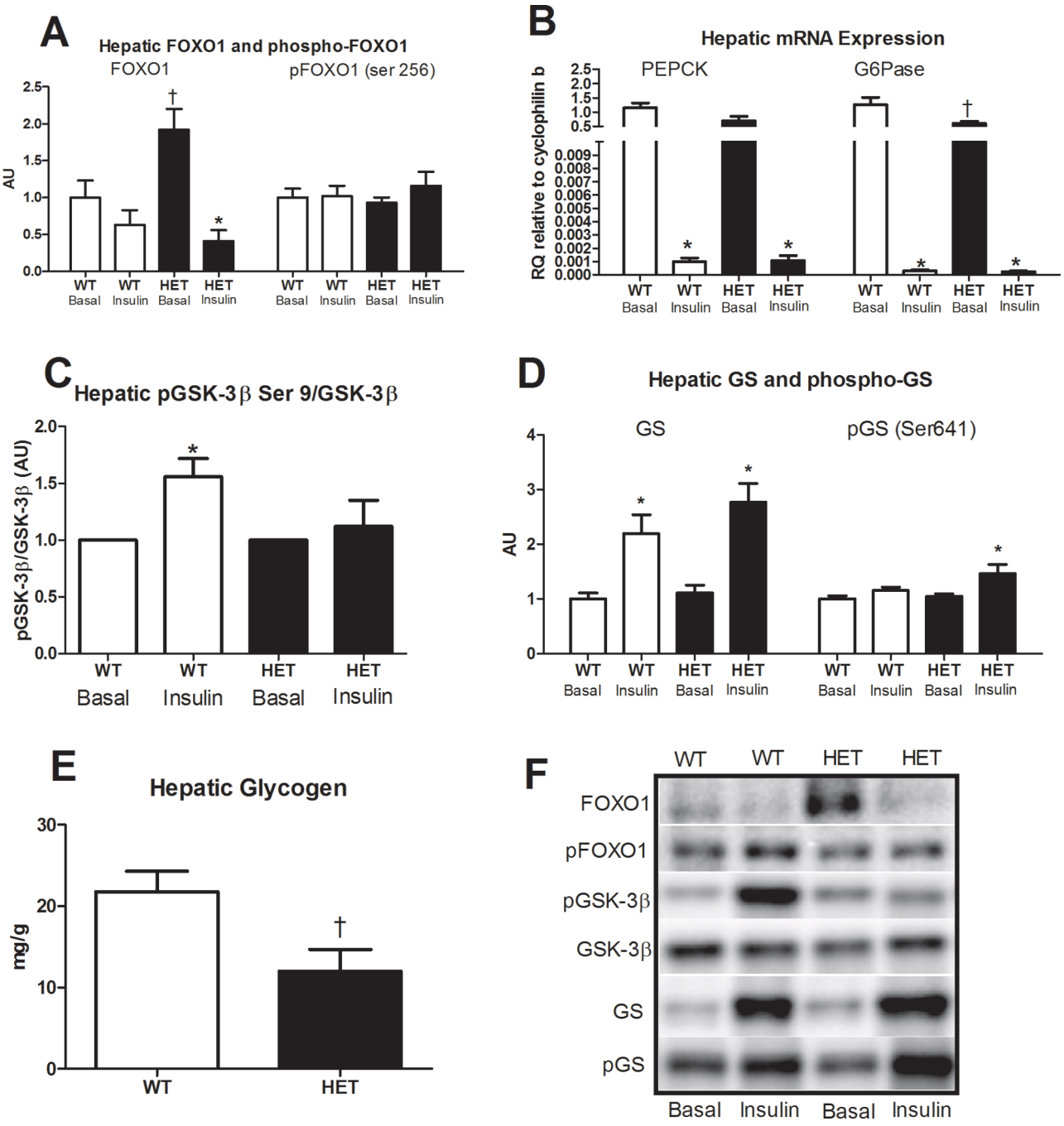

Figure 4.

Factors involved in hepatic gluconeogenesis and glycogen metabolism in HET MTP and WT mice. Basal and insulin-stimulated hepatic FOXO1 and phospho-FOXO1 protein content (Figure 4A), basal and insulin-stimulated mRNA expression of PEPCK and G6Pase (Figure 4B), basal and insulin-stimulated phosphorylation status of GSK-3β (Figure 4C), basal and insulin-stimulated phosphorylation status of GS (Figure 4D) and hepatic glycogen content following hyperinsulinemic-euglycemic clamp (Figure 4D). * Significantly different than basal, $p<0.05$. † Signicantly different from WT under same condition, $p<0.05$. Representative Western blots shown in Figure 5F.

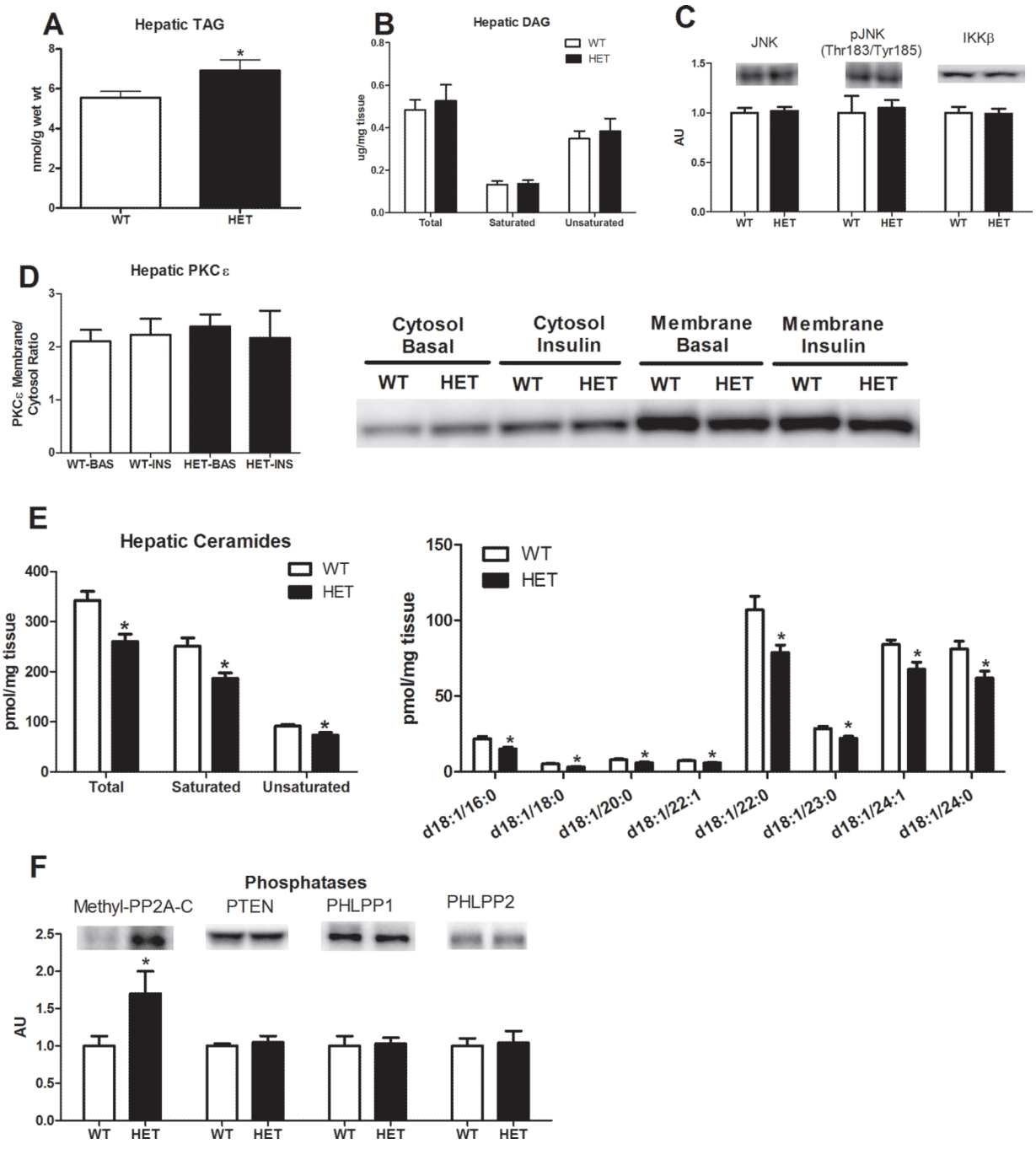

Figure 5.

Hepatic TAGs, DAGs, JNK activation, PKCε activation status, ceramide species, and protein content of protein phosphatases in HET MTP and WT mice. Hepatic TAG content (Figure 5A); total, saturated, and unsaturated hepatic DAG content (Figure 5B); hepatic JNK, phospho-JNK, and IKKβ protein content (Figure 5C), basal and insulin-stimulated PKCε protein content either in the cytosol or in the membrane fraction (Figure 5D), total ceramide content (saturated and unsaturated) and individual ceramide molecular species (Figure 5E), and hepatic protein content of protein phosphatases (Figure 5F). Values are means ± SE (n=8–12 per group; 9–10 per group for ceramide analyses). * Significantly different than WT under same condition, $p<0.05$.

Table 1

Animal, serum, and liver characteristics

Variable	WT	HET
Body weight (g)	36.75±0.77	33.63±0.94*
Fat pad mass (g)	1.07±0.10	0.85±0.07*
Food consumption (g/wk)	31.45±0.52	32.59±1.35
Serum TAG (mg/dL)	67.8±3.9	60.5±3.9
Serum FFAs (μmol/L)	223.1±12.7	202.2±12.1
Serum β-hydroxy-butyrate (μmol/L)	171.0±16.7	159.3±13.4
Serum glucose (mg/dL)	180.9±6.0	183.4±6.2
Serum insulin (ng/mL)	1.00±0.1	0.94±0.11
Serum ALTs (U/L)	30.7±1.7	30.1±3.3
Liver SOD-1 activity (U/mg)	26.3±3.2	24.6±2.2
Liver catalase activity (μmoles/min/μg)	1.63±0.16	1.70±0.11
Liver β-HAD activity (nmol/min/μg)	17.4±1.3	17.1±1.5
Liver CSA (nmol/min/μg)	93.4±2.7	88.7±1.9

Values are means ± SE (n=8–12).

*Significantly different than WT, $p<0.05$. TAG = triacylglycerol; FFAs = free fatty acids; ALT = alanine aminotransferase; β-HAD = β-hydroxyacyl-CoA dehydrogenase; CSA = citrate synthase activity; SOD = superoxide dismutase.